Expression of flowering locus T2 transgene from Pyrus communis L. delays dormancy and leaf senescence in Malus×domestica Borkh, and causes early flowering in tobacco.

Freiman A, Golobovitch S, Yablovitz Z, **Belausov E**, Dahan Y, Peer R, Avraham L, Freiman Z, Evenor D, Reuveni M, Sobolev V, Edelman M, Shahak Y, Samach A, Flaishman MA.

Plant Sci. 2015 Dec;241:164-76.

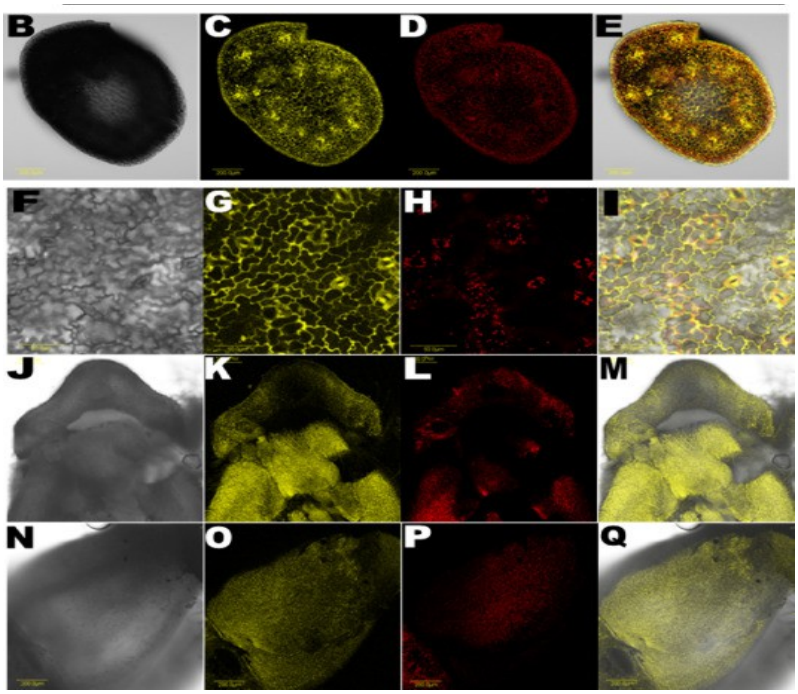

Presence of YFP in different organs of transgenic apple constitutively expressing *PcFT2–YFP* gene. (b–e) Cross section of 35S::*PcFT2–YFP* tissue-cultured shoot. (f–i) Leaf. (j–m) Apical bud. (n–q) Lateral bud. (b, f, j, n) Bright-field image; (c, g, k, o) yellow fluorescence corresponding to chimeric PcFT2–YFP; (d, h, l, p) red fluorescence corresponding to chlorophyll autofluorescence; (e, i, m, q) confocal image recorded simultaneously for yellow and bright-field image.

Dissecting the contribution of microtubule behaviour in adventitious root induction.

Abu-Abied M, Rogovoy Stelmakh O, Mordehaev I, Grumberg M, Elbaum R, Wasteneys GO, Sadot E.

J Exp Bot. 2015 May;66(9):2813-24.

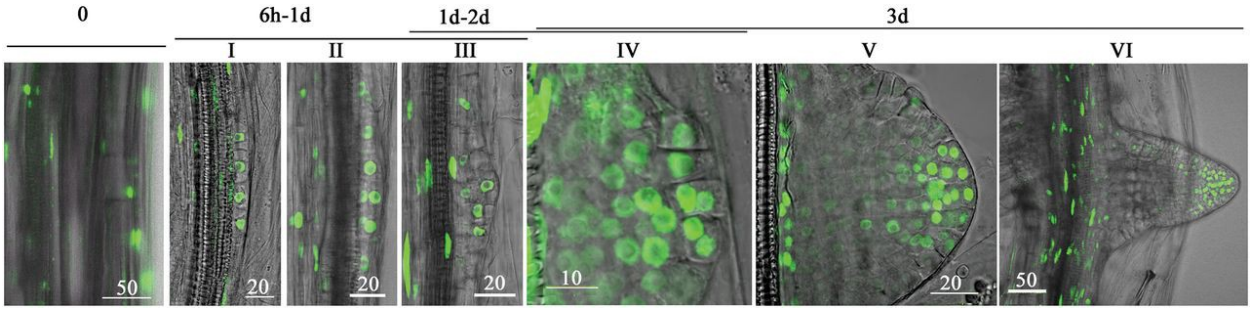

The seven stages of AR formation. Hypocotyls (5–6mm in length) of $DR5_{pro}$:venus-expressing plants were excised from etiolated seedlings and incubated in MS with 1% sucrose and 10 μM K-IBA. Initial stages of AR formation were imaged at the indicated time periods. Stage 0: before root induction. Stage I: four founder cells are formed after anticlinal cell division. Stage II: the first periclinal cell division occurs to create two layers. Stages III, IV and V: more periclinal and anticlinal cell divisions occur to create 3–4, 5–8, and 9–15 cell layers, respectively. Stage V: the primordium acquires the classical dome like shape. Stage VI: root emergence.

Cell-cycle progress in obligate predatory bacteria is dependent upon sequential sensing of prey recognition and prey quality cues.

Rotem O, Pasternak Z, Shimoni E, **Belausov E**, Porat Z, Pietrokovski S, Jurkevitch E.

Proc Natl Acad Sci U S A. 2015 Nov 3;112(44)

.

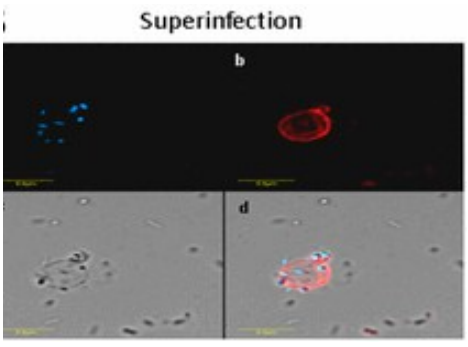

Confocal microscopy rendering of numerous AP cells penetrating a ghost cell under high multiplicity of infection (5:1 predator:ghost ratio). (*a*) DAPI stain. (*b*) FM4-64 membrane stain. (*c*) Bright-field imaging. (*d*) Composite of *a*–*c*.

Analysis of Microtubule-Associated-Proteins during IBA-Mediated Adventitious Root Induction Reveals KATANIN Dependent and Independent Alterations of Expression Patterns.

Abu-Abied M, Mordehaev I, Sunil Kumar GB, Ophir R, Wasteneys GO, Sadot E.

PLoS One. 2015 Dec 2;10(12)

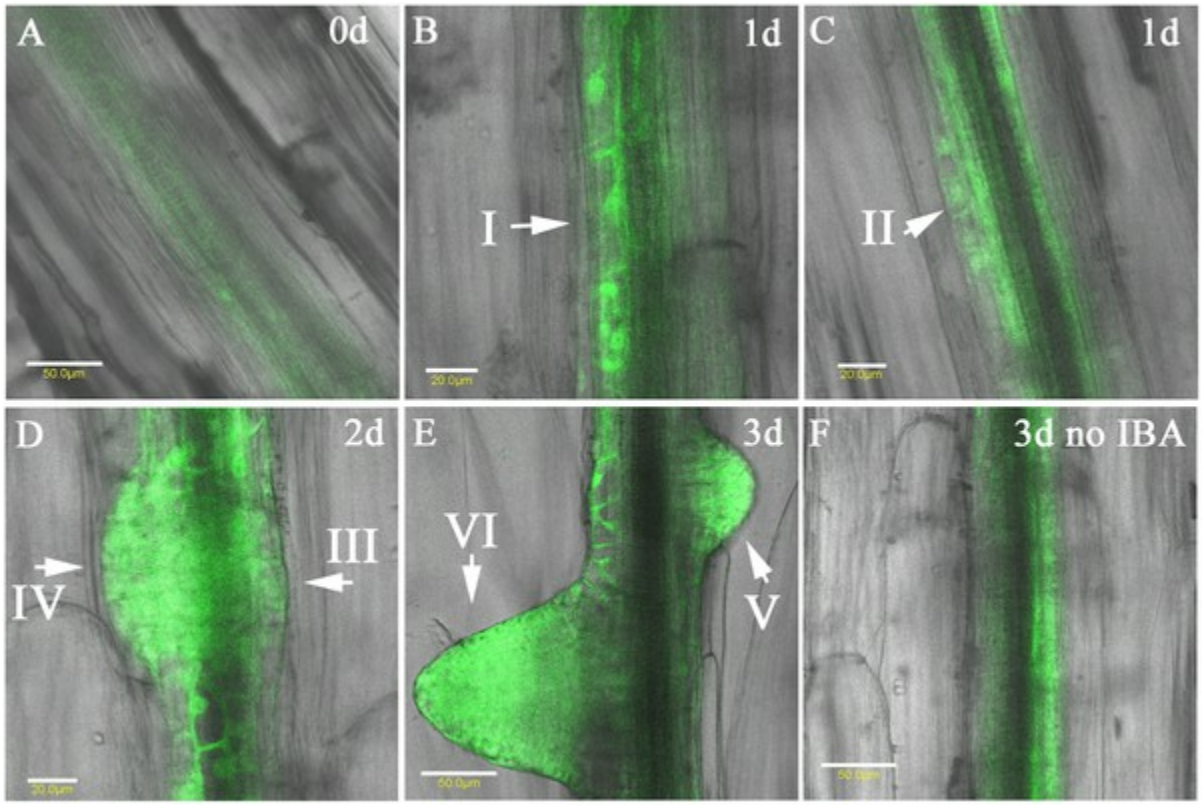

Expression of GFP under the *MOR1*$_{prom}$ during AR induction.

Influx and Efflux of Strigolactones Are Actively Regulated and Involve the Cell-Trafficking System.

Fridlender M, Lace B, Wininger S, Dam A, Kumari P, **Belausov E**, Tsemach H, Kapulnik Y, Prandi C, Koltai H.

Mol Plant. 2015 Dec 7;8(12)

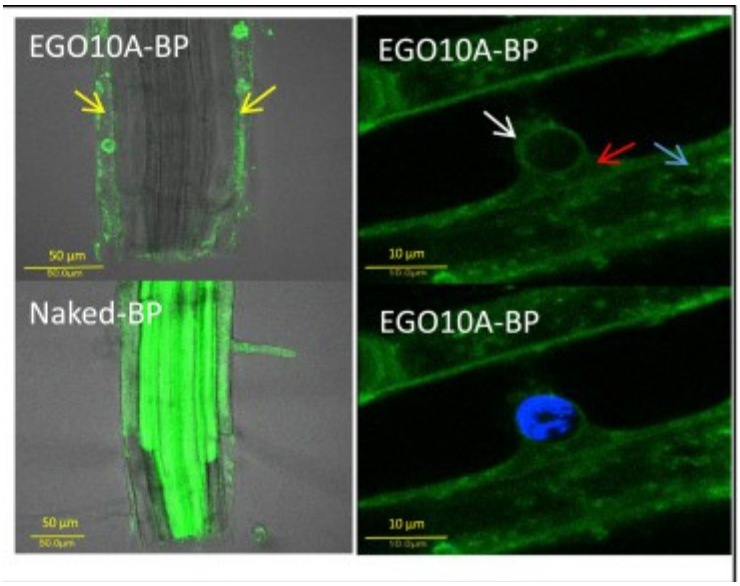

Images of roots treated with EGO10A-BP or naked-BP. Green indicates EGO10A-BP or naked-BP signal, blue indicates DAPI staining. Yellow arrows denote the epidermis cell layer. Blue, red, and white arrows indicate EGO10A-BP staining in endosome-like bodies, cytoplasm, and nucleus envelope, respectively.

Development of a fluorescent in situ hybridization (FISH) technique for visualizing CGMMV in plant tissues.

Shargil D, Zemach H, **Belausov E**, Lachman O, Kamenetsky R, Dombrovsky A.

J Virol Methods. 2015 Oct;223:55-60.

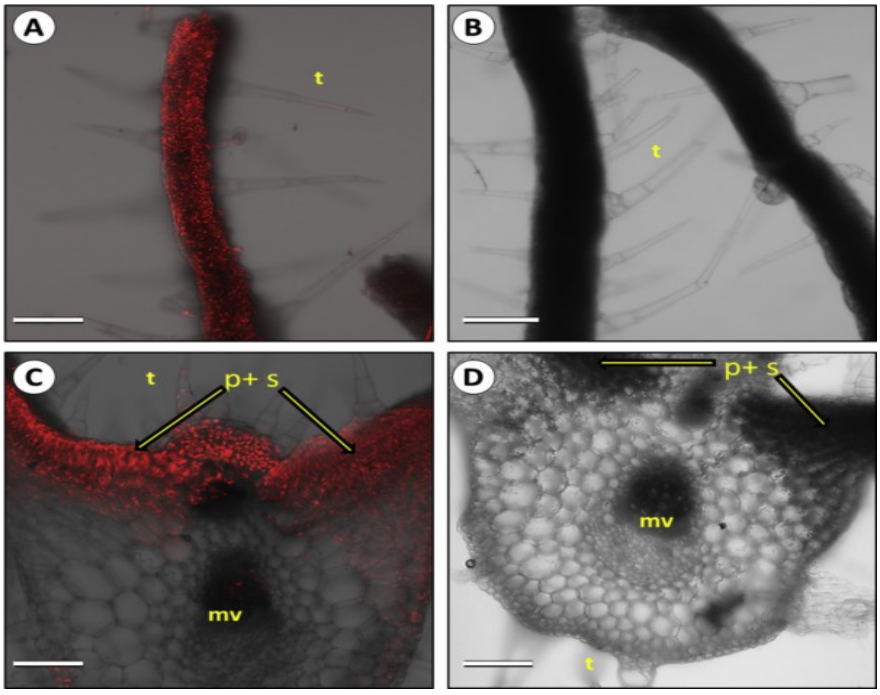

Representative confocal microscopy images of fluorescent *in situ* hybridization labeling (Cy-3, 10 pmol) of Cucumber green mottle mosaic virus (CGMMV) in a male flower of an infected *C. melo* (cv. Raanan) plant. (A) Transverse section of an anther with pollen grains; (B) transverse section of an anther of a healthy plant with pollen grains. [Bar = 100 μm.].

The Tomato yellow leaf curl virus V2 protein forms aggregates depending on the cytoskeleton integrity and binds viral genomic DNA.

Moshe A, **Belausov E**, Niehl A, Heinlein M, Czosnek H, Gorovits R.

Sci Rep. 2015

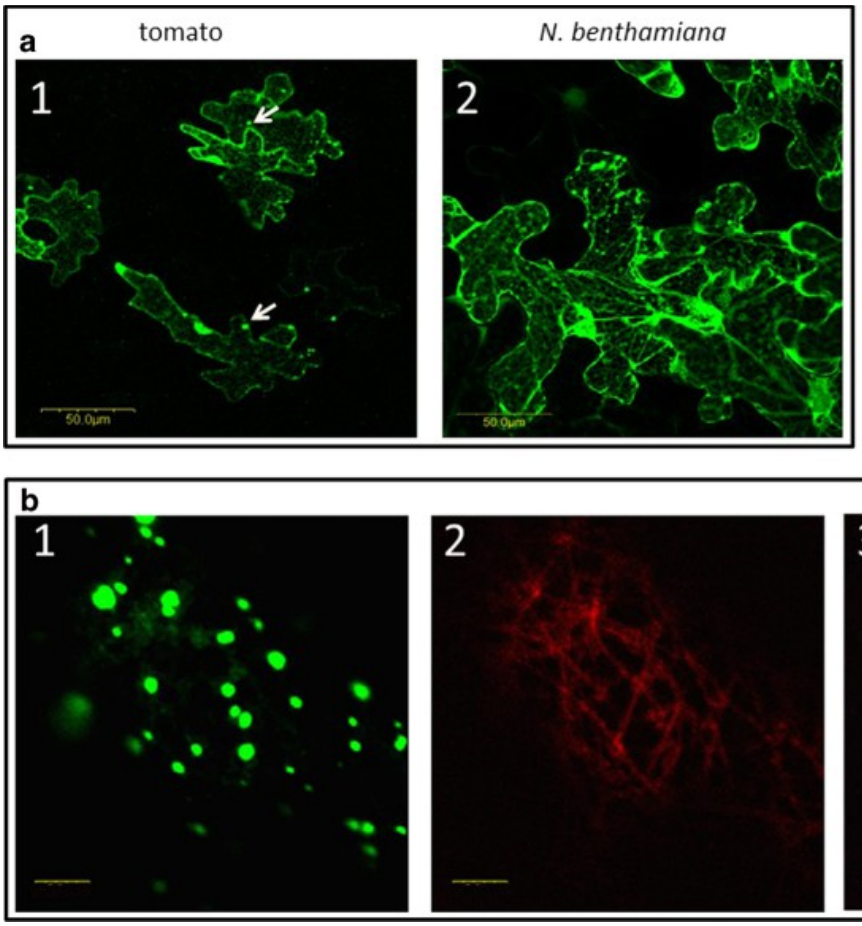

Expression of fusion V2:GFP in epidermal cells of tomato and *N. benthamiana* leaves. **a**: tomato (1) and *N. benthamiana* (2) leaves infiltrated with *A. tumefaciens* carrying the V2:GFP expression plasmid. Bar: 50 µm. **b**: *N. benthamiana* leaves infiltrated with A. tumefaciens carrying the V2:GFP and MAP4:RFP expression plasmids: 1. V2:GFP (green); 2. microtubule marker MAP4:RFP (red); 3. merge of V2:GFP and MAP4:RFP, V2 co-localization with microtubules is indicted in yellow. Bar: 5 µm.

TYLCV-Is movement in planta does not require V2 protein.

Hak H, Levy Y, Chandran SA, **Belausov E**, Loyter A, Lapidot M, Gafni Y.
Virology. 2015 Mar;477:56-60

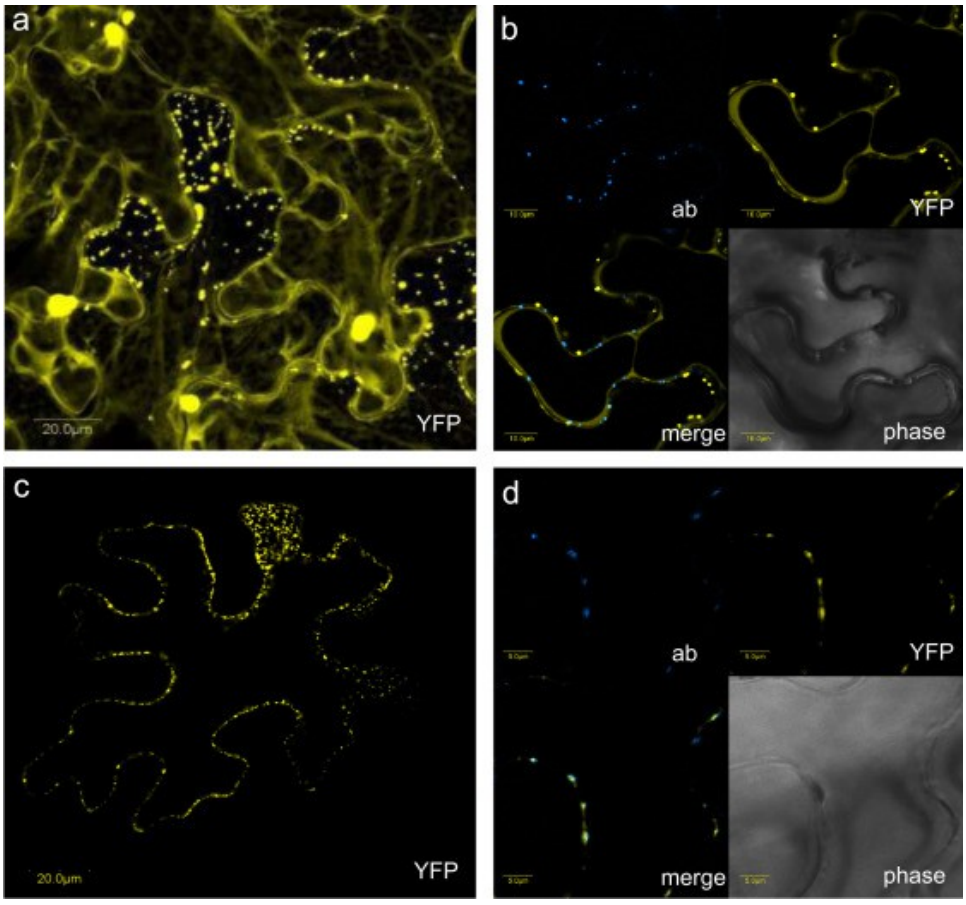

Intracellular localization of TYLCV-Is V2 and C4. (a) YFP-V2 expressed in agroinfiltrated *N. benthamiana*leaf is located around the nucleus, in microbodies throughout the cytoplasm, and in association with cytoplasmic strands. The image is a projection of several confocal sections. (b) YFP-V2 expressed in agroinfiltrated *N. benthamiana* leaf along with aniline blue-stained plasmodesmata. (c) YFP-C4 expressed in agroinfiltrated *N. benthamiana* leaf is found in a spotted pattern at the cell periphery. (d) YFP-C4 expressed in agroinfiltrated *N. benthamiana* leaf along with aniline blue-stained plasmodesmata. YFP signal is shown in yellow, aniline blue (ab) signal is shown in blue. Plastid autofluorescence was filtered out.

Arabidopsis response to low-phosphate conditions includes active changes in actin filaments and PIN2 polarization and is dependent on strigolactone signalling.

Kumar M, Pandya-Kumar N, Dam A, Haor H, Mayzlish-Gati E, **Belausov E**, Wininger S, Abu-Abied M, McErlean CS, Bromhead LJ, Prandi C, Kapulnik Y, Koltai H.

J Exp Bot. 2015 Mar;66(5):1499-510

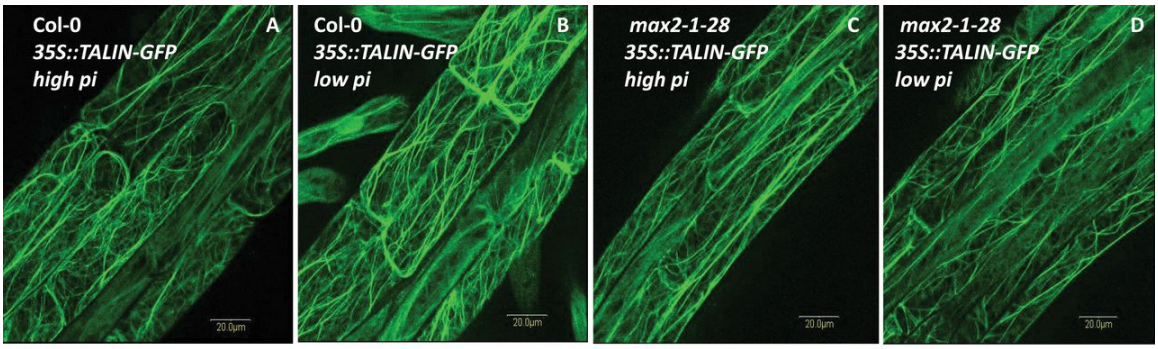

Bundling of TALIN–GFP F-actin in the epidermal cells of the primary-root elongation zone in 35S::TALIN–GFP roots of seedling grown under high (2mM) and low (1 µM) Pi conditions (48 HPG). (A–D) TALIN–GFP signal in Col-0 (A, B) or *max2-1* mutant (*max2-1–28*; C, D) grown under high- or low-Pi conditions.

Abscission of flowers and floral organs is closely associated with alkalization of the cytosol in abscission zone cells.

Sundaresan S, Philosoph-Hadas S, Riov J, **Belausov E**, Kochanek B, Tucker ML, Meir S.
J Exp Bot. 2015 Mar;66(5):1355-68.

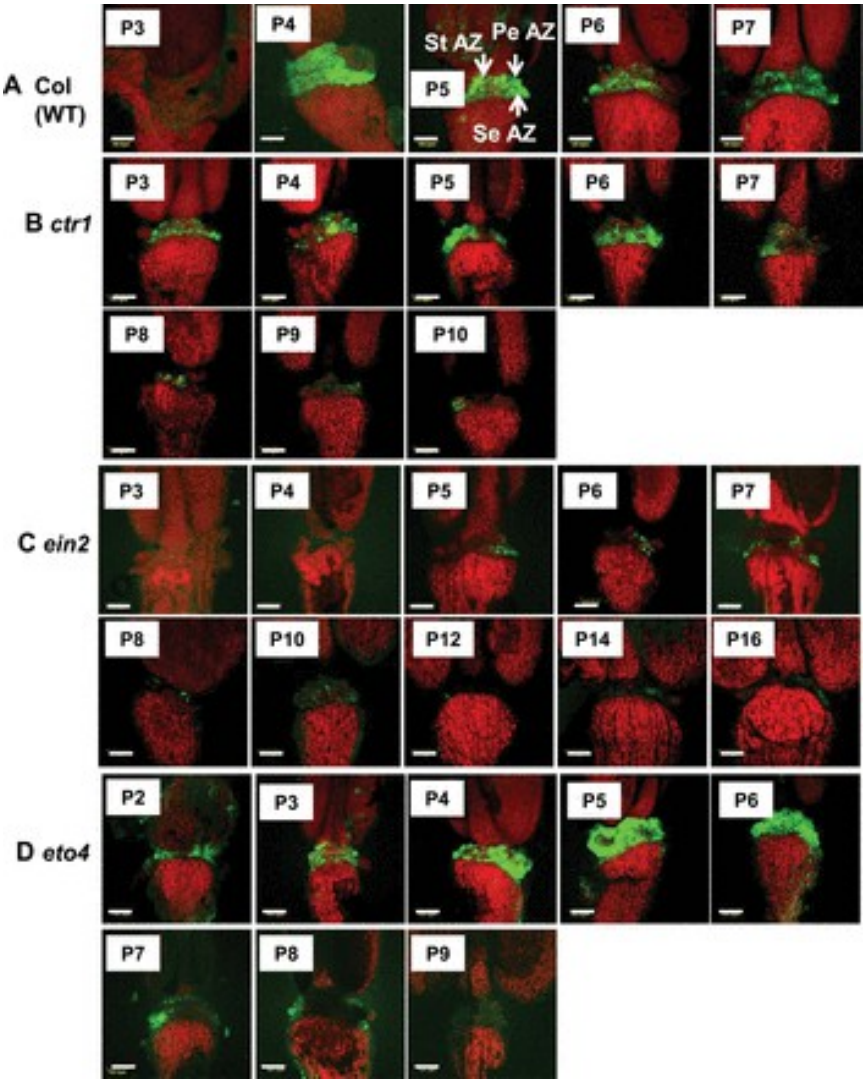

Fluorescence micrographs of BCECF images of flower organ AZ of *Arabidopsis* Col WT (A) and Arabidopsis ethylene-related mutants *ctr1* (B), *ein2* (C), and *eto4* (D), showing pH changes in P3–16 flowers.

The PH gene determines fruit acidity and contributes to the evolution of sweet melons.

Cohen S, Itkin M, Yeselson Y, Tzuri G, Portnoy V, Harel-Baja R, Lev S, Sa'ar U, Davidovitz-Rikanati R, Baranes N, Bar E, Wolf D, Petreikov M, Shen S, Ben-Dor S, Rogachev I, Aharoni A, Ast T, Schuldiner M, **Belausov E**, Eshed R, Ophir R, Sherman A, Frei B, Neuhaus HE, Xu Y, Fei Z, Giovannoni J, Lewinsohn E, Tadmor Y, Paris HS, Katzir N, Burger Y, Schaffer AA.

Nat Commun. 2014 Jun 5;5:4026.

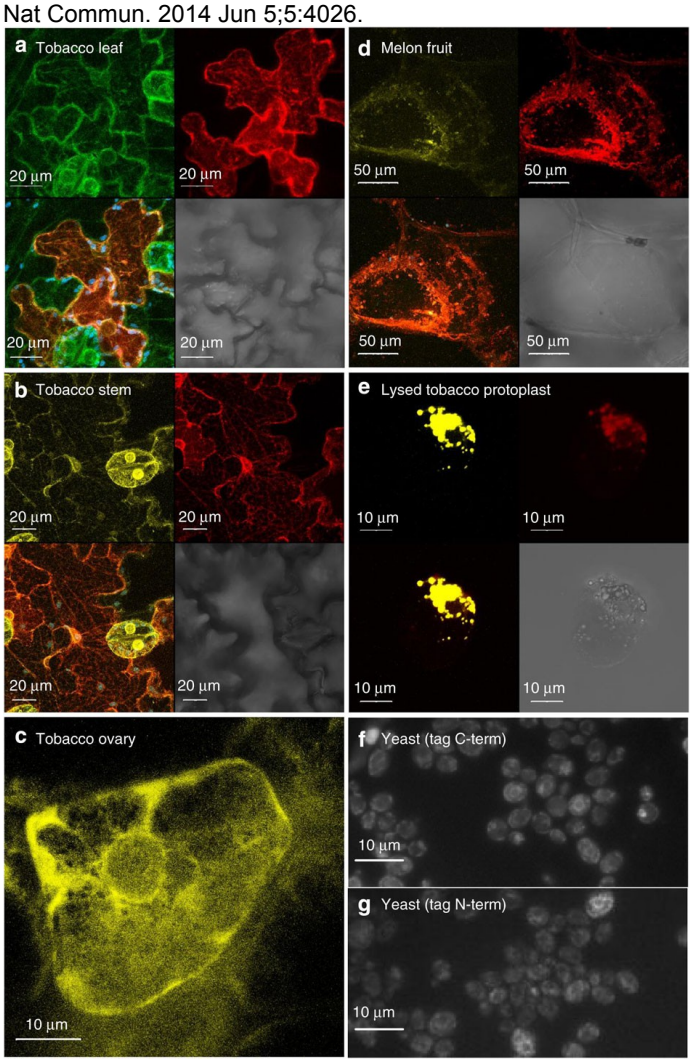

(**a**–**e**) YFP-PH or PH-GFP (yellow amino-terminal fluorescent tag or green carboxy-terminal fluorescent tag, respectively) expression in stable transgenic tobacco. (**a**) Tobacco leaf epidermal cells; (**b**) stem cells; (**c**) immature ovary; (**d**) transient YFP-PH and HDEL-RFP coexpression in young melon fruit. The micrograph of melon fruit is a three-dimensional reconstruction; (**e**) YFP-PH (yellow) in lysed tobacco protoplasts showing the fluorescence in the cytoplasmic components attached to the vacuole but not on the tonoplast membrane; (**f**) C-terminal fluorescent tag imaged in WT yeast cells (lens × 100). (**g**) N-terminal fluorescent tag imaged in WT yeast cells (lens × 100). In both **f** and **g**, PH is targeted to the endoplasmic reticulum, as is evident from the double ring-like pattern visualized in the yeast. In composite figures **a**,**b**,**d** and **e**, PH with fluorescent tag is dyed in yellow or green (top left corner), transient HDEL-RFP expression in red (top right corner), the combined fluorescence in orange (bottom left corner) and clear field in grey (bottom right corner).

Fluorescence in situ hybridizations (FISH) for the localization of viruses and endosymbiotic bacteria in plant and insect tissues.

Kliot A, Kontsedalov S, Lebedev G, Brumin M, Cathrin PB, Marubayashi JM, Skaljac M, **Belausov E**, Czosnek H, Ghanim M.

J Vis Exp. 2014 Feb 24;(84)

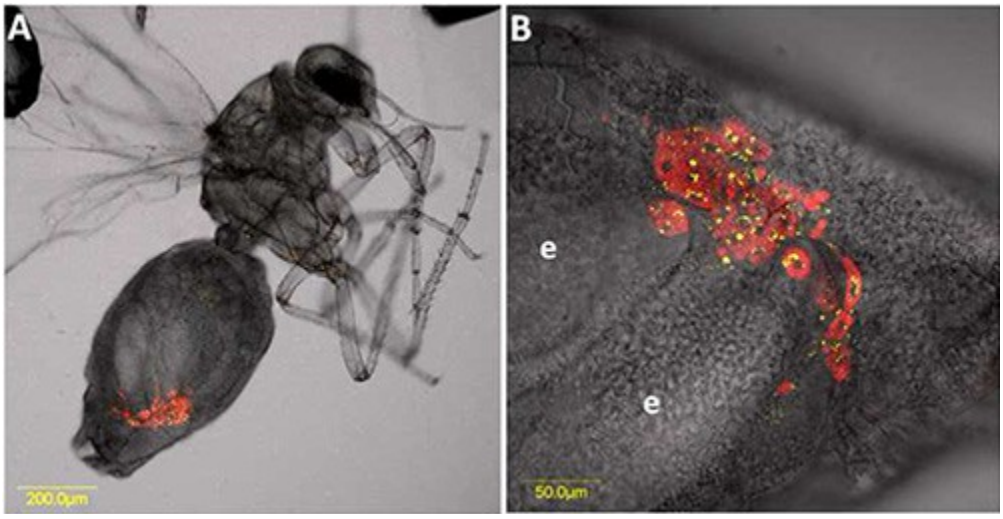

Double FISH of *Portiera* and *Arsenphonus* on *B. tabaci* Q biotype adult (**A**) and zoom on the labeled area (**B**) both under bright field
channel and combined optical sections detecting the fluorescent signals emitted by each probe. *Portiera*-specific probe (red) conjugated to Cy5
and *Arsenphonus*-specific probe (yellow) conjugated to Cy3 were used. e: egg.

Strigolactone analog GR24 triggers changes in PIN2 polarity, vesicle trafficking and actin filament architecture.

Pandya-Kumar N, Shema R, Kumar M, Mayzlish-Gati E, Levy D, Zemach H,**Belausov E**, Wininger S, Abu-Abied M, Kapulnik Y, Koltai H.

New Phytol. 2014 Jun;202(4):1184-96

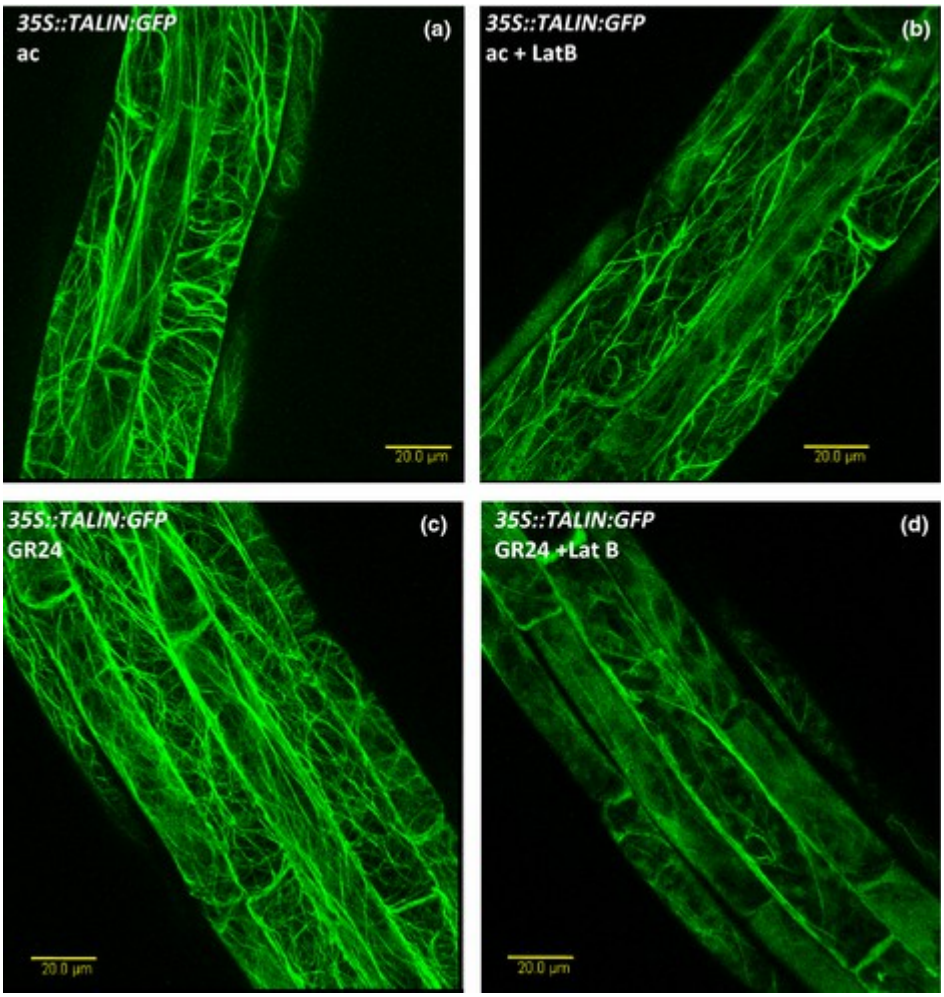

Sensitivity of TALIN-GFP F-actin in the epidermal cells of the primary root elongation zone to latrunculin B (LatB) treatment in 35S::TALIN-GFP *Arabidopsis thaliana* seedlings grown on acetone or GR24 plates (72–96 h postgermination). (a–d) TALIN-GFP signal in roots of Col-0 seedlings grown on acetone (ac; a, b) or GR24 (c, d) plates (bars, 20 µm) and treated (b, d) or not treated (a, c) with LatB.

Structural and functional differences between pheromonotropic and melanotropic PK/PBAN receptors.

Hariton-Shalev A, Shalev M, Adir N, **Belausov E**, Altstein M.

Biochim Biophys Acta. 2013 Nov;1830(11):5036-48

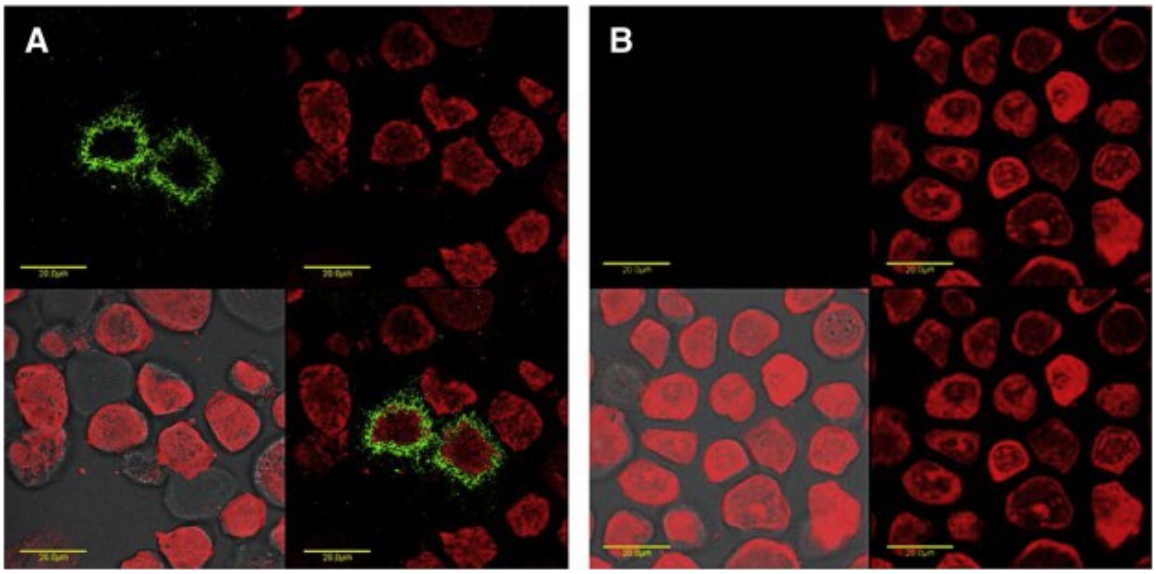

Immunostaining of *Hep*- and *Spl*-PK/PBAN-R stably expressed in *Sf9* cells. *Spl*-PK/PBAN-R-transfected cells stained with anti-PK/PBAN-R antiserum (A); *Spl*-PK/PBAN-R-transfected cells stained with PI serum (B).

Hexokinase mediates stomatal closure.

Kelly G, Moshelion M, David-Schwartz R, Halperin O, Wallach R, Attia Z, **Belausov E**, Granot D.

Plant J. 2013 Sep;75(6):977-88.

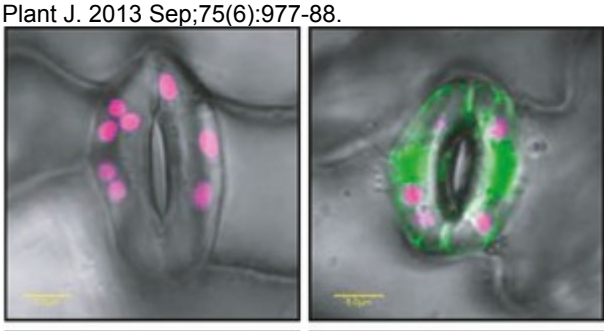

Expression of GFP under the control of the *KST1* promoter is specific to guard cells.

mCSF1, a nucleus-encoded CRM protein required for the processing of many mitochondrial introns, is involved in the biogenesis of respiratory complexes I and IV in Arabidopsis.

Zmudjak M, Colas des Francs-Small C, Keren I, Shaya F, **Belausov E**, Small I, Ostersetzer-Biran O.

New Phytol. 2013 Jul;199(2):379-94

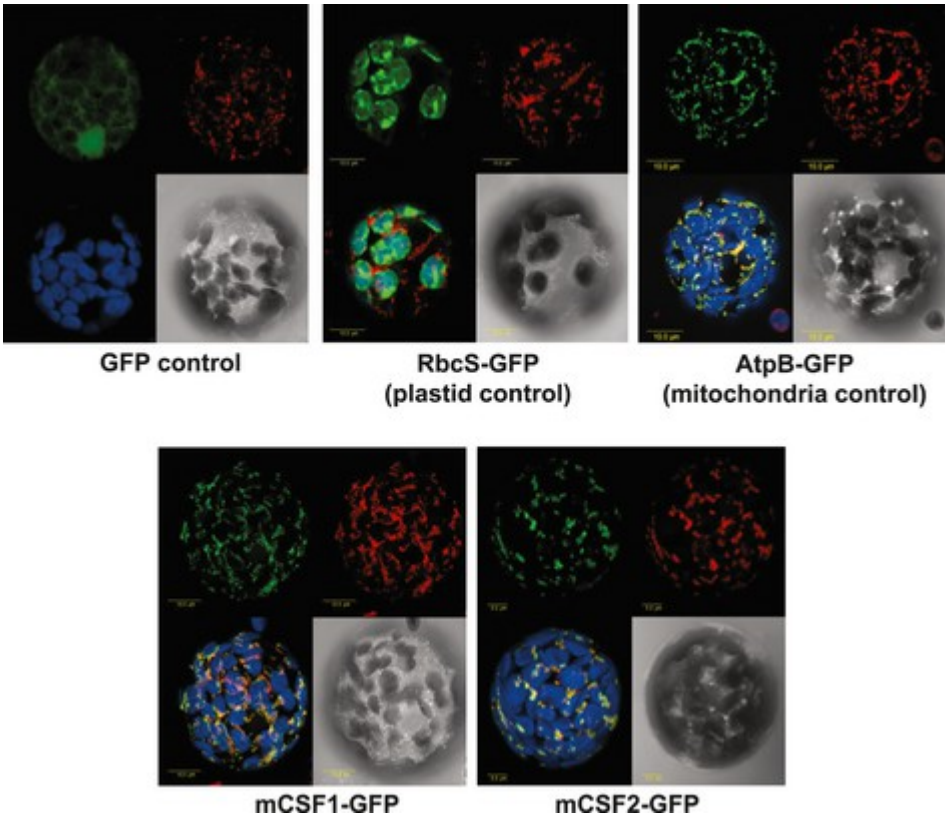

Localization of mitochondrial CAF-like splicing factor 1–green fluorescent protein (mCSF1-GFP) fusion protein to mitochondria. Tobacco protoplasts were transformed with expression plasmids encoding GFP fused to the N-termini of Rubisco small subunit (RbcS, 65 amino acids), mitochondrial AtpB (mAtpB, 54 amino acids), and the N-termini regions of Arabidopsis mCSF1 and mCSF2 paralogs (Table 1). For each construct, images are shown of GFP (green, upper left panel), MitoTracker (red, upper right panel), merged images with chlorophyll autoflorescence (blue, lower left panel), and light microscopy (lower right panel).

Identification of Salmonella enterica genes with a role in persistence on lettuce leaves during cold storage by recombinase-based in vivo expression technology.

Kroupitski Y, Brandl MT, Pinto R, **Belausov E**, Tamir-Ariel D, Burdman S, Sela Saldinger S.
Phytopathology. 2013 Apr;103(4):362-72.

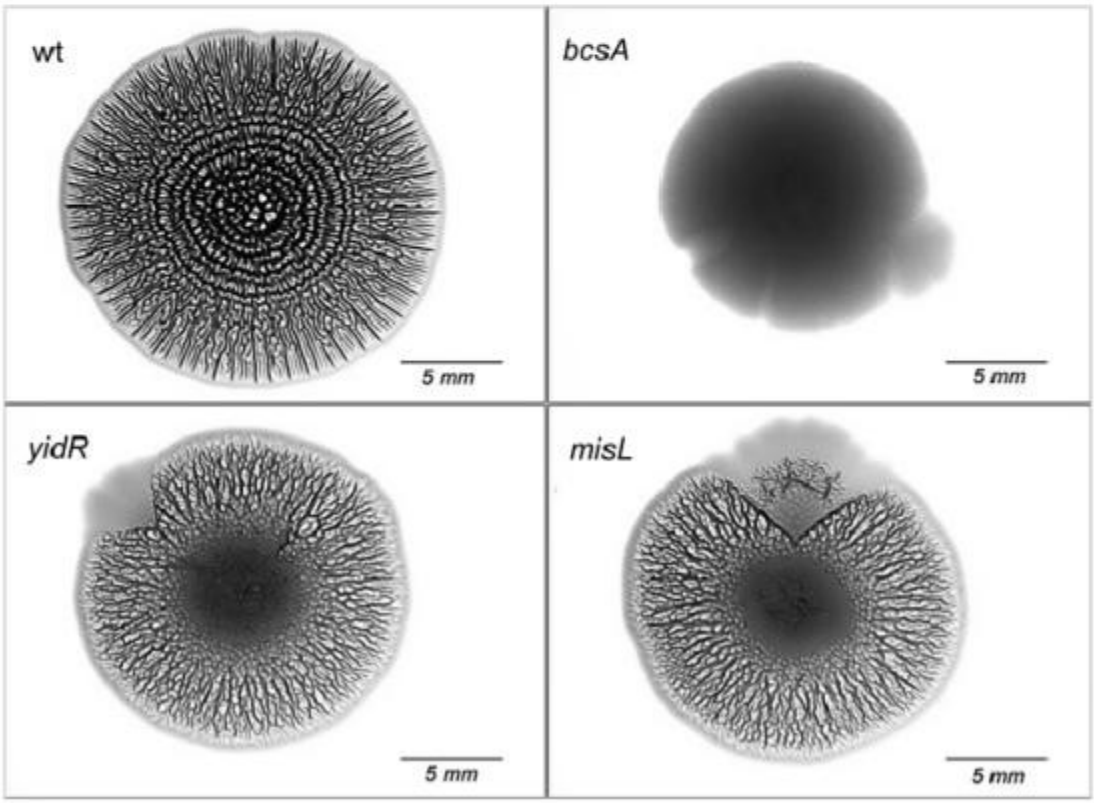

Biofilm formation and colony morphology of Salmonella enterica wild-type (wt) and mutants.

Strigolactone signaling in the endodermis is sufficient to restore root responses and involves SHORT HYPOCOTYL 2 (SHY2) activity.

Koren D, Resnick N, Mayzlish Gati E, **Belausov E**, Weininger S, Kapulnik Y, Koltai H.
New Phytol. 2013 May;198(3):866-74.

Enantioselective effects of (+)- and (-)-citronellal on animal and plant microtubules.

Altshuler O, Abu-Abied M, Chaimovitsh D, Shechter A, Frucht H, Dudai N, Sadot E.

J Nat Prod. 2013 Sep 27;76(9):1598-604.

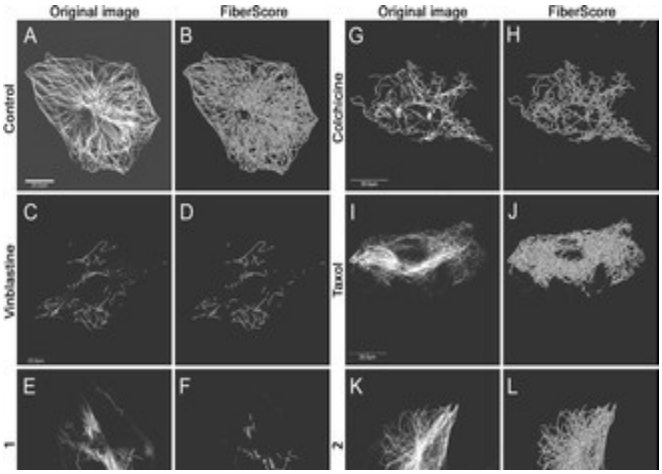

Quantitative analysis of the effects of **1** and **2** on MTs. Ref52 cells were treated for 30 min with 0.1 μM colchicine or vinblastine, 2 μM paclitaxel, or 27.5 μM **1** or **2**. The cells were fixed and stained for MTs. Images were analyzed by FiberScore for total fluorescence associated with fibers. A, C, E, G, I, and K are the images of MTs. B, D, F, H, J, and L show the fibers scored by the software. Scale bar = 20 μm.